



The
University
Of
Sheffield.

This is a repository copy of *Differential expression of VEGFA isoforms regulates metastasis and response to anti-VEGFA therapy in sarcoma*.

White Rose Research Online URL for this paper:

<https://eprints.whiterose.ac.uk/116514/>

Version: Accepted Version

Article:

English, W.R. orcid.org/0000-0003-3024-2441, Lunt, S.J., Fisher, M. et al. (8 more authors) (2017) Differential expression of VEGFA isoforms regulates metastasis and response to anti-VEGFA therapy in sarcoma. *Cancer Research*, 77 (10). pp. 2633-2646. ISSN 0008-5472

<https://doi.org/10.1158/0008-5472.CAN-16-0255>

Reuse

Items deposited in White Rose Research Online are protected by copyright, with all rights reserved unless indicated otherwise. They may be downloaded and/or printed for private study, or other acts as permitted by national copyright laws. The publisher or other rights holders may allow further reproduction and re-use of the full text version. This is indicated by the licence information on the White Rose Research Online record for the item.

Takedown

If you consider content in White Rose Research Online to be in breach of UK law, please notify us by emailing eprints@whiterose.ac.uk including the URL of the record and the reason for the withdrawal request.

Differential Expression of VEGFA Isoforms Regulates Metastasis and Response to Anti-VEGFA Therapy in Sarcoma

William R. English*, Sarah Jane Lunt, Matthew Fisher, Diane V. Lefley, Mohit Dhingra, Yu-Chin Lee, Karina Bingham, Jack E. Hurrell, Scott K. Lyons^{1,2}, Chryso Kanthou and Gillian M. Tozer.

Tumor Microcirculation Group, Department of Oncology and Metabolism, University of Sheffield School of Medicine, Beech Hill Road, Sheffield, S10 2RX, UK. ¹CR-UK Cambridge Institute, The Li Ka Shing Building, Robinson Way, Cambridge, CB2 0RE, UK.

²Current address: Cold Spring Harbor Laboratory, One Bungtown Road Cold Spring Harbor, NY 11724, USA.

*Corresponding Author: Email: w.english@sheffield.ac.uk. Tumor Microcirculation Group, Department of Oncology and Metabolism, University of Sheffield School of Medicine, Beech Hill Road, Sheffield, S10 2RX, UK.

Running Title: VEGFA isoforms regulate metastasis and response to therapy

Key Words: VEGF, isoform, metastasis, VEGFR1, sarcoma

Financial Support: WRE, SJL, MF, DVL, KB, JEH, CK and GMT received support from Cancer Research UK (program grant C1276/A9993), Yorkshire Cancer Research (equipment grant S311) and the University of Sheffield. MD was supported by a fellowship from the Jean Shanks Foundation.

Word count excluding references: 8070. Total number of Figures: 7

Conflict of Interest: The authors of this manuscript have no actual, potential, or perceived conflict of interest with regard to the manuscript submitted for review.

Abstract: Elevated plasma concentrations of soluble VEGFA isoforms are associated with poor prognosis in parallel with improved response to treatment with the anti-VEGFA antibody bevacizumab. To uncover the underlying mechanism to these observations, we administered anti-VEGFA therapy to mice bearing luminescent mouse fibrosarcomas expressing single VEGFA isoforms or their wild type counterparts expressing all isoforms (fs120, fs164, fs188 or fsWT). Expression of the more soluble isoforms conferred an advantage for lung metastasis from subcutaneous tumors (fs120/164 versus fs188/WT); fs120 cells also produced more lung colonies than fs188 cells when injected intravenously. Metastasis from subcutaneous fs120 tumors was more sensitive than fs188 to treatment with the anti-VEGFA antibody B20-4.1.1. Despite elevated plasma levels of VEGFA in fs120 tumor-bearing mice and a dependence on VEGF receptor 1 activity for metastasis to the lung, B20-4.1.1 did not affect survival in the lung on intravenous injection. B20-4.1.1 inhibited subcutaneous tumor growth and decreased vascular density in both fs120 and fs188 tumors. However, migration of fs120, but not fs188 cells *in vitro* was inhibited by B20-4.1.1. The greater survival of fs120 cells in the lung was associated with VEGFR1-dependent accumulation of CD11b positive myeloid cells and higher expression of the VEGFR1 ligand, PIGF2, by the fs120 cells *in vitro* and in the plasma and lungs of fs120 tumor-bearing mice. We conclude that soluble VEGFA isoform expression increases fibrosarcoma metastasis through multiple mechanisms that vary in their sensitivity to anti-VEGF/VEGFR inhibition, with VEGFA-targeted therapy suppressing metastasis through effects on the primary tumor rather than the metastatic site.

Introduction

Vascular endothelial growth factor A (VEGFA) is a potent regulator of neovascularization that contributes to tumor growth and metastasis via its receptors VEGFR1/Flt-1, VEGFR2/KDR, and VEGFR3. The function-blocking antibody for VEGFA, bevacizumab (Avastin®), and several small molecule VEGFR inhibitors are now in clinical use (1). However, VEGFA targeted therapies have not achieved universal success and one of the remaining challenges is to identify biomarkers enabling prospective selection of the most appropriate patients for treatment (2).

VEGFA exists as multiple isoforms generated through alternative splicing and proteolysis (3,4). This generates forms of VEGFA that are either freely diffusible/soluble (e.g. VEGF121 and 110) or bound by different degrees to the extracellular matrix (ECM) that limits diffusion (e.g. VEGF165, 189, 206). Recent retrospective analyses of data from several large phase III clinical trials have found a link between high concentrations of soluble VEGFA isoforms in plasma and poor prognosis, but also improved response to bevacizumab (Avastin®), where progression free survival (PFS) was measured (5-9). However, little is known about underlying mechanisms. Pre-clinical studies have shown that tumor cell expression of VEGF120 (mouse equivalent of human VEGF121) influences vascular development during embryonic development, and also response to therapy in tumors *in vivo* (10-13). In tumors, VEGF120 expression promotes the formation of leaky vasculature, with low pericyte coverage and high interstitial fluid pressure (IFP) (13); characteristics that are linked to increased metastasis, the key factor regulating patient survival (14,15).

In this study, we directly investigated the putative link between expression of soluble VEGFA isoforms, metastasis and response to VEGFA-targeted therapy in mouse models of fibrosarcoma, utilizing tumor cells engineered to express only single isoforms of VEGFA. For fibrosarcoma cells expressing the more soluble VEGFA isoforms, and VEGF120 in particular, mice with subcutaneous tumors had increased plasma VEGFA and lung metastasis that was sensitive to anti-VEGFA therapy. Our data indicate anti-VEGFA therapy predominantly inhibits metastasis through effects on the primary tumor, as survival within the lung following intravenous injection of VEGF120 expressing tumor cells was insensitive to anti-VEGFA therapy. However, survival of VEGF120 expressing tumor cells in the lung after intravenous injection was strongly dependent on VEGFR1 activity. PIGF2 was identified as a potential VEGFR1 ligand mediating these effects in VEGF120 expressing tumor cells.

Materials and Methods

Detailed materials and methods can be found within the supplementary methods section.

Sources and breeding of mice. All experiments were conducted in accordance with the United Kingdom Home Office Animals (Scientific Procedures) Act 1986, local ethical approval and recently published guidelines (16). CB17-SCID (CB17/*Icr-Prkdcscid/IcrIcoCrl*) mice were obtained from Charles River, UK, and maintained as colony at the University of Sheffield. C57Bl6/SCID (B6.CB17-*Prkdcscid/SzJ*) mice were obtained from Charles River (UK). C57BL6/J VEGFR1- Δ TKD mice, (17) were generously provided by Prof. M Shibuya (Tokyo Medical and Dental University, Japan) via Dr KH Plate (Johan Goethe University Medical School, Germany). These were crossed to generate C57Bl6/SCID mice homozygous for *vegfr1* or *vegfr1- Δ TKD* (VEGFR1-WT and VEGFR1- Δ TKD mice respectively).

In vivo models of tumor growth and metastasis. The majority of experiments were conducted in C57Bl6/SCID mice. Experiments examining the effect of B20-4.1.1 and cediranib were conducted in CB-17-SCID mice. Levels of lung metastasis from subcutaneous tumors or survival of cells on intravenous injection were not found to be significantly different between the two strains of mice (unpublished data). Mouse fibrosarcoma cell lines expressing either VEGF120, 164 or 188 (fs120, fs164, fs188 respectively) or all isoforms (fsWT) have been described previously and were derived from day 13.5 embryos from a mixed Swiss background and retrovirally transformed with hRAS and SV40 (12). Variants expressing luciferase 2 (fs120-LS, fs164-LS, fs188-LS and fsWT-LS) for optical

imaging were developed as described in Supplementary Methods. Cell lines were cultured from passage 8 after authentication in house (morphology, VEGFA isoform expression, SV40 and hRAS expression levels) to a maximum of passage 30 (typically 2 – 3 months). Subcutaneous tumors were established by injection of 10^6 cells into the rear dorsum of mice. For treatment with control IgG (BE5) or anti-VEGFA (B20-4.1.1) (Genentech Inc. San Francisco, USA (18,19)), tumors were grown to 200 mm^3 and mice treated with 5 mg/kg antibody twice weekly by intraperitoneal injection up to a maximum end-point tumor size of 1000 mm^3 . For an experimental model of metastasis involving intravenous injection of tumor cells, mice were injected with 5×10^4 cells into a tail vein and tumor cell arrest within the lung capillary network or survival or colonization of cells in lung tissue investigated at 5 min, 48h or ≥ 21 days after injection respectively. In each case, presence of tumor cells in lung tissue was determined by analysis of luciferase activity or immuno-staining, as described below.

Analysis of luciferase activity in vivo and ex vivo. Mice were injected ip with D-luciferin (Perkin Elmer) and bioluminescence of the thoracic region was measured using an IVIS Lumina II (Perkin Elmer) imaging system. Alternatively, mice were killed and individual lobes of excised lungs were imaged. Bioluminescence output measured as photons per second per cm^2 of tissue that radiate into a solid angle of one steridian ($\text{p/s/cm}^2/\text{sr}$) or as photon per second (p/s) was calculated using Living Image™ software (Perkin Elmer). For analysis of luciferase activity in lung lysates, luciferase activity was measured, corrected for protein content and activity expressed as $\text{p/s}/\mu\text{g}$ protein.

Immunohistochemistry, immunofluorescence and analysis of vascular density.

Tumors were formalin-fixed and paraffin wax embedded (FFPE) or frozen in OCT and sectioned. Staining for CD31 in FFPE sections and manual counts of vascular density were performed as described previously (13). CD34 and α -Smooth Muscle Actin (α SMA) immunofluorescence staining of FFPE sections was used to establish the percent of vessels associated with perivascular cells. α SMA positive cells were counted as perivascular if they were in direct contact with CD34 positive vascular staining and adopted a flattened and/or elongated morphology. Anti-CD34 rather than anti-CD31 was used in combination with the α SMA in FFPE sections for technical reasons. CD31 and CD34 staining of the vasculature were found to overlap almost completely in frozen sections and provide virtually identical estimates of vascular density (Supplementary Figure S1). For immunofluorescent staining of SV40 (fibrosarcoma cells), CD11b, Ki67, phospho S139- γ H2AX, CD31, laminin and collagen-I, frozen sections were cut and stained after methanol/acetone fixation. Detailed methods can be found in the supplementary section.

Measurement of VEGFR1 ligand expression. Lysates from 3D multicellular fs120 or fs188 cell spheroids were analyzed on mouse angiogenesis protein profiler arrays (R&D Systems). Spot intensity for PIgf2, VEGFA and VEGFB was quantified using enhanced chemi-luminescence (ECL) on a C-digit® blot scanner (LiCor, Cambridge) and Image Studio (LiCor, Cambridge). PIgf2 levels were further characterised in plasma, tumors and lung homogenates of tumor bearing animals using an anti-mouse PIgf2 ELISA (R&D Systems).

In vitro analysis of tumor ECM and cell migration. Tumors were homogenized in cell lysis buffer and proteins separated using SDS-PAGE before collagen-I and laminin were detected using Western blot and ECL. Laminin and collagen-I were measured using densitometry and normalized with respect to GAPDH. Migration of serum-starved cells was measured across 8 µm pore membranes coated on the upper surface with laminin or collagen-I towards serum in the presence of control IgG or B20-4.1.1. Prior to analysis of single cell migration using live video microscopy, cellular adhesion was titrated against coating concentrations of laminin and collagen to ensure maximal adhesion was reached. Live video microscopy of single cell migration was performed in the presence or absence of the function blocking anti-mouse and human VEGFA antibody B20-4.1.1 or control IgG BE5 on laminin or collagen-I coated plastic. Speed and distance migrated was calculated as described in detail in the supplementary methods section.

Statistical analysis. Data were plotted and analyzed using GraphPad Prism 6.0e (GraphPad Prism Software Inc). Pair-wise analysis was made using an unpaired Student's t-test with a Welch's correction and a Mann-Whitney test for parametric and non-parametric data. For parametric analysis of grouped data, ANOVA followed by a Sidak's multiple comparison test was used. For non-parametric data a Kruskal-Wallis test followed by a Dunn's multiple comparison test was used. Kaplan Meier analysis was used to measure significance between times to reach a pre-determined humane end point as a surrogate for survival. In some experiments, data were combined from more than one cohort of mice to reach statistical power and to ensure similar data were obtained from separate

litters. Where data were combined from more than cohort, they were normalized against the mean of a common parameter before statistical analysis; see figure legends for details.

Results

Expression of the more soluble isoforms of VEGFA is associated with increased fibrosarcoma metastasis to the lung.

Metastasis was assessed in whole lungs excised from mice bearing subcutaneous tumors after inoculation with fs120-LS, fs164-LS or fs188-LS cells, or their wild type counterparts expressing all VEGFA isoforms (fsWT-LS), at the end-point size of approximately 1000 mm³ (Fig 1A). Luciferase activity in lung lysates showed that mice bearing fs120-LS tumors had significantly higher levels of metastasis than those bearing fsWT-LS or fs188-LS tumors (Fig 1A); lung luminescence was 10 to 20-fold higher for fs120-LS than for fsWT-LS or fs188-LS ($P < 0.001$ and $P < 0.05$ respectively). Metastasis for fs164-LS was closest to fs120-LS, with lung luminescence significantly higher than for fsWT-LS (Fig 1A, $P < 0.01$). Differences in metastasis were not due to differences in time from tumor inoculation to end-point as this was very similar between the different tumor lines with only fsWT-LS tumors taking a slightly longer time to reach end point (Fig 1B). In all subsequent studies, we focused on comparing the fs120-LS and fs188-LS cells, as they represent the extremes of soluble versus ECM bound isoforms.

To confirm that tumor cells could colonize the lung and develop macro-metastatic deposits, we injected tumor cells intravenously as an experimental model of metastasis. In this case, colonization of the lungs by tumor cells could be detected by bioluminescent imaging of live mice (Fig 1C), in addition to imaging of excised intact lung lobes (Fig 1D). Consistent with metastasis from the primary subcutaneous tumor, bioluminescence within the thoracic regions of

mice injected intravenously with fs120-LS cells was detected at significantly higher levels than in mice injected with fs188-LS cells by day 21 after injection ($P < 0.01$, Fig 1E). Mice injected intravenously with fs120-LS cells reached a pre-determined humane end-point ($>10^7$ photons per second (p/s) within the thoracic region), significantly sooner than mice injected with fs188-LS cells ($P < 0.05$, Fig 1F). At day 40, the majority of fs120-LS injected mice had reached their humane end-point (8/9) whereas only 5/10 of fs188-LS injected mice had reached the end point by day 50 (Fig 1F).

Lung metastasis from subcutaneous fs120-LS tumors is sensitive to both B20-4.1.1 treatment and host VEGFR1 tyrosine kinase activity.

We then investigated whether the anti-mouse/human VEGFA function-blocking recombinant antibody B20-4.1.1, directed to amino acids 8 – 109 of VEGFA that are common to both VEGF120 and VEGF188, (18,19), had variable effects on metastasis dependent on differential tumor cell expression of VEGFA isoforms. Mice bearing subcutaneous fs120-LS or fs188-LS tumors were treated with B20-4.1.1 when tumors reached approximately 200 mm³, and lungs were removed when subcutaneous tumors reached the end-point size of 1000 mm³. B20-4.1.1 decreased metastasis to the lung from fs120-LS tumors significantly (3-fold, $P < 0.05$), but had no significant effect on metastasis from fs188-LS tumors (Fig 2A).

Mice with subcutaneous fs120-LS tumors had higher plasma concentrations of VEGFA than mice with fs188-LS tumors ($P < 0.05$; Fig 2B). Since circulating VEGFA could act at sites of VEGF receptor expression in the host, we investigated whether there was a role for VEGF receptor 1 (VEGFR1) in the elevated lung

metastasis observed from subcutaneous fs120-LS versus fs188-LS tumors, as activity of VEGFR1 in host cells has been shown to be involved in the early stages of lung colonization (20,21). For this, tumor cells were injected subcutaneously into mice with inactivated VEGFR1, due to a deleted tyrosine kinase domain (VEGFR1-ΔTKD mice), or into VEGFR1-WT control mice (17) and metastasis measured as before. The time taken for subcutaneous fs120-LS or fs188-LS tumors to reach 1000 mm³ and tumor vascular density were not significantly different between VEGFR1-WT and VEGFR1-ΔTKD mice (Supplementary Fig S2A – S2C). However, lung metastasis from subcutaneous fs120-LS tumors was significantly decreased by approximately 5-fold ($P < 0.05$) when cells were injected into VEGFR1-ΔTKD mice compared with VEGFR1-WT mice (Fig 2C). In contrast, inactivation of VEGFR1 had no significant effect on lung metastasis from subcutaneous fs188-LS tumors, with a tendency towards an increase rather than a decrease (Fig 2C).

In order to investigate whether VEGFA (via B20-4.1.1 treatment) and VEGFR1 activity affect survival within the lung after tumor cells have entered the circulation, we injected fs120-LS or fs188-LS tumor cells intravenously via the tail vein of mice and measured bioluminescence of excised lung lobes 48 h later. As we found for metastasis from subcutaneous tumors (Fig 2C), intravenous injection of fs120-LS cells into VEGFR1-ΔTKD mice decreased lung bioluminescence by approximately 5-fold compared with VEGFR-WT mice ($P < 0.01$, Fig 2D and 2E), whereas lung bioluminescence following intravenous injection of fs188-LS cells was unaffected by host activity of VEGFR1 (Fig 2E). Lung bioluminescence at 48 h following intravenous injection of fs188-LS cells

was lower than that for fs120-LS cells ($P < 0.01$) in the wild-type mice (Fig 2E), as we had previously found at 21 days (Fig 1E) and for metastasis from the subcutaneous tumors (Fig 1A and 2A). Overall, the pattern of lung bioluminescence observed following intravenous injection of fs120-LS and fs188-LS cells into wild-type or VEGFR1- Δ TKD mice was very similar to that found for metastasis from subcutaneous tumors (comparing Figs 2E and C). Coupled to the lack of an obvious influence of VEGFR1 on the subcutaneous primary tumor itself (Supplementary Fig S2), these data suggest that fs120-LS survive better than fs188-LS cells in lung tissue within the first 48 h, at least partially via a VEGFR1-dependent mechanism, which could account for their differing metastatic rates from subcutaneous inoculation of cells.

In contrast to the influence of VEGFR1 activity, B20-4.1.1 treatment had no influence on fs120-LS survival in the lung 48 h after intravenous injection (Fig 2F). This suggests that a VEGFR1 ligand, other than VEGFA itself, is involved in promoting survival of tumor cells in the lung. Furthermore, it suggests that the inhibitory effect of B20-4.1.1 on metastasis from subcutaneous tumors (Fig 2A) is via effects on the primary subcutaneous tumor.

Pre-existing subcutaneous fs120 but not fs188 tumors increase survival of intravenously injected tumor cells in the lung

Although our data examining tumor cell survival in the lung 48 h after intravenous injection suggested that innate characteristics of the fs120-LS cells themselves are important for their increased lung metastasis over fs188-LS, the full metastatic process could also be influenced by additional factors arising from

the primary tumor. To address this, mice were first injected subcutaneously with fibrosarcoma cells lacking luciferase expression (fs120 or fs188). When tumors reached approximately 200 mm³, counterpart fs120-LS or fs188-LS luciferase-expressing cells were injected intravenously, followed by measurement of bioluminescence in excised lungs after 48 h, as before (Fig 3A). In this case, lung bioluminescence following intravenous injection of tumor cells into wild-type mice was approximately 150-fold higher for fs120-LS cells versus fs188-LS cells (Fig 3A), compared with an approximate 5-fold differential when there was no subcutaneous tumor present (Fig 2E). Secreted factors and/or early cellular dissemination from fs120-LS subcutaneous tumors could have a priming effect on lung tissue, resulting in a favorable environment for survival of the intravenously injected tumor cells. By analyzing lung homogenates from a cohort of mice bearing small 200 mm³ subcutaneous tumors, we found that fs120-LS tumor cells had already disseminated to the lungs at this stage (Supplementary Fig S3A). In contrast, pre-treatment of mice with fs120 cell-conditioned medium prior to intravenous injection of fs120-LS cells was unable increase cell survival in the lung (Supplementary Fig S3B).

Survival of intravenously injected fs120-LS cells (but not fs188-LS) in the lung, when a primary subcutaneous tumor was present, still showed dependence on VEGFR1 activity (Fig 3A). Similar to data obtained on intravenous injection of fs120-LS cells alone, B20-4.1.1 treatment did not inhibit survival of intravenously-injected fs120-LS cells in the lung in the presence of a subcutaneous tumor (Fig 3B). This provides further support for the notion that blocking the activity of

VEGFA within the primary tumor is the main mechanism by which B20-4.1.1 reduced lung metastasis from subcutaneous fs120-LS tumors (Fig 2A).

Since B20-4.1.1 had no effect on survival of intravenously injected tumor cells in the lung, we investigated whether VEGFR1 ligands, other than VEGFA itself, were preferentially produced by fs120-LS cells. Using a protein array-based method to screen lysates from multicellular spheroids of tumor cells (22), fs120 cells were found to express significantly higher levels of the VEGFR1 ligand PIGF2 than fs188 cells. VEGFA and VEGFB spot intensity was low and showed no significant differences between the cell lines (Supplementary Fig S4A – S4B). The increased expression of PI GF2 was confirmed using ELISA of cell conditioned medium, with fs120 cells expressing significantly more PI GF2 than fs188 cells under hypoxic conditions (Fig 3C). Although PI GF2 was not differentially expressed between fs120-LS and fs188-LS subcutaneous tumors (Supplementary Fig S4C), mice bearing fs120-LS tumors did have significantly higher levels of PI GF2 in plasma and lungs than those bearing fs188-LS tumors ($P < 0.05$; Fig 3D and E). Since both VEGFA and PI GF2 concentrations in plasma were increased in fs120-LS tumor bearing mice, this points to redundancy in activation of VEGFR1 in host tissue by VEGF-family ligands, which would explain why B20-4.1.1 did not decrease survival of intravenously injected fs120-LS cells in the lung.

B20-4.1.1 decreases vascular density and tumor growth in both fs120-LS and fs188-LS tumors

Considering the evidence for B20-4.1.1 acting at the primary tumor site to decrease lung metastasis selectively from fs120-LS tumors, we investigated

whether B20-4.1.1 had a VEGFA isoform-selective effect on subcutaneous tumor growth, vascular density or pericyte coverage that could account for this effect. B20-4.1.1 retarded tumor growth to a very similar extent in fs120-LS and fs188-LS tumor types (Fig 4A-C). We found significant anti-vascular activity for B20-4.1.1 in both tumor types, as determined by CD31-positive ($CD31^{+VE}$) blood vessel counts, but no differential effect between the two tumor types. Specifically, vascular density was significantly reduced by approximately 2-fold in both fs120-LS and fs188-LS tumors ($P < 0.001$ and $P < 0.01$ respectively, Fig 4D and E). There was a tendency for the percent of α SMA pericyte positive (α SMA $^{+VE}$) vessels to increase in fs120-LS tumors following B20-4.1.1 treatment but effects were insignificant in both tumor types (Fig 4F and 4G). Pericyte positive vessels were more numerous ($P < 0.01$) in control fs188-LS tumors than in control fs120-LS tumors (Fig 4G), confirming previous results for subcutaneous tumors of non-bioluminescent cells (12).

fs120-LS tumors express high levels of laminin and fs120 cell migration on laminin is inhibited by B20-4.1.1.

Since we did not identify any VEGFA isoform specific effects of B20-4.1.1 on blood vessels within the primary subcutaneous tumors, we investigated their extracellular matrix (ECM) composition, as this has an influential role in regulating cell migration and metastasis (23). fs120 cells have higher levels of adhesion and spreading on laminin compared to collagen-I *in vitro* and they adopt a mesenchymal morphology on laminin versus collagen-I, suggesting increased migration on this matrix (24). Tumors derived from fs188 cells also have higher numbers of α SMA-positive fibroblasts than those from fs120 cells

(12), suggestive of differences in ECM composition between the two tumor types *in vivo* (25). Analysis of protein extracted from subcutaneous tumor lysates using western blot showed that fs120-LS tumors expressed higher total levels of laminin compared to fs188-LS tumors with the reverse true for collagen-I (Fig 5A and 5B). Laminin could be detected in protein extracts of fs120 and fs188 cell cultures *in vitro*. Collagen-I was detected in protein extracts of fs188 cells as high molecular weight aggregates that were absent in fs120 cell extracts. Lower molecular weight immunoreactive bands for collagen-I were detected at low levels in lysates of fs120 cells but these did not align with immuno-reactive forms seen in fs188 cells or pooled tumor lysates, indicating fs120 cell do not make detectable levels of collagen-I (Supplementary Fig S5). Immunofluorescence staining of tumors showed laminin is associated with the vasculature in both tumor types with very prominent intense staining in fs188-LS tumors (Fig 5C) consistent with increased vascular maturation associated with greater α SMA positive pericyte coverage (Fig 4G and (12)). However, laminin was expressed more widely throughout the fs120-LS tumor stroma and with a greater staining intensity in comparison with fs188-LS tumors, accounting for the differences seen on western blots between the two tumor types (Fig 5C). Collagen-I was partially associated with the vasculature in fs188-LS tumors but also more widely distributed, whereas there was negligible collagen-1 staining in fs120-LS tumors (Figure 5D).

We then investigated migration of fs120 and fs188 cells on laminin versus collagen-I matrices and its dependency on VEGFA using B20-4.1.1. Using transwells coated with collagen-I or laminin on the upper surface, serum starved fs120 cells migrated more extensively towards the serum-containing bottom

chamber than fs188 cells on laminin, whereas fs188 cells were more migratory on collagen-I (Fig 5E and 5F). B20-4.1.1 inhibited fs120 cell migration on laminin but not on collagen-I coated membranes and had no significant effect on migration of fs188 cells on either matrix (Fig 5E and 5F). We also investigated single cell migration on laminin or collagen-I coated plastic in the presence of serum measured using live video microscopy, so that migration could be quantified more accurately and independently of chemotactic effects. In this case, fs188 cell migration speed and distance was found to be very similar on laminin and collagen and faster than fs120 cell migration on both matrices (Supplementary Fig S6A and S6B). However, as for the transwell assay, only fs120 cell migration on laminin could be inhibited by B20-4.1.1 (Supplementary Fig S6A and S6B).

Vascular arrest of intravenously injected fs120-LS cells in the lung is higher than that of fs188-LS cells

We next sought to investigate how fs120-LS cells gain a survival advantage over fs188-LS cells in the lung during the first 48 h after intravenous injection. We found that bioluminescence of fs120-LS cells in the lung was significantly higher than fs188-LS cells even at 5 minutes post-injection (4-fold; $P < 0.01$; Fig 6A). Lung bioluminescence significantly decreased by 48 h in both cell types by 400-700 fold ($P < 0.01$; Fig 6A), with a similar differential between the cell types at 48 h (6-fold; $P < 0.01$; Fig 6A) as previously observed (see Fig 2E). Immunofluorescence staining of lung sections to detect the SV40 positive ($SV40^{+VE}$) fibrosarcoma cells directly confirmed significantly fewer fs188-LS cells compared to fs120-LS cells at 5 min, with the majority still trapped within the

vasculature, indicating differences in efficiency of vascular arrest within the lung ($P < 0.05$; Fig 6B and 6C). VEGFR1 activity had no significant influence on cell numbers within the lung at 5 min (Fig 6B). SV40 staining of fs120-LS and fs188-LS cells showed sub-populations of tumor cells that were highly distorted and disrupted, as well as more rounded cells (Fig 6C), suggesting cancer cell trauma on encountering the microvasculature of the lung (26). To investigate whether there was a difference between the cell types, we measured γ H2AX phosphorylation (p- γ H2AX) in SV40^{+VE} nuclei by immunofluorescence staining (Fig 6D) to detect activation of the DNA damage response pathway in response to mechanical trauma or nuclear deformation (27). We found that fewer fs120-LS cells were positive for nuclear p- γ H2AX than fs188-LS cells at 5 min ($P < 0.05$, Fig 6E) and this was independent of VEGFR1 activity (Fig 6E). Immunofluorescence staining of lungs of mice 48 h after intravenous injection of cells for Ki67, a marker of proliferation, showed an increase in Ki67/S40 double positive fs120-LS cells, (Fig 6F), compared to fs188-LS cells ($P < 0.01$, Fig 6G). These results demonstrate that fs120-LS cells can survive initial arrest in the vasculature of the lung better and subsequently proliferate more efficiently than fs188-LS cells.

Accumulation of CD11b cells in the lung was higher after intravenous injection of fs120-LS cells than fs188-LS cells and was associated with VEGFR1 activity

CD11b antigen positive (CD11b^{+VE}) leucocyte recruitment is an early event that supports survival of cells during metastasis and has been shown to require stromal activity of VEGFR1 (28). 5 min after intravenous injection of fs120-LS or fs188-LS cells, no increase in total numbers of CD11b^{+VE} cells was detected

compared to control lungs and there was no difference between VEGFR-WT and Δ TKD mice (Fig 7A). CD11b^{+VE} cells clustered around fs120-LS and fs188-LS cells equally in the lungs of mice at 5 min (Supplementary Fig S7A and 7B). At 48 h, CD11b^{+VE} cell counts were significantly increased in lungs containing fs120-LS cells in VEGFR1-WT mice ($P < 0.001$) but not in VEGFR1- Δ TKD mice (Fig 7A). Conversely, injection of fs188-LS cells did not increase the levels of CD11b^{+VE} cells in the lungs at 48 h and there was no dependence on the VEGFR1 TKD status of the mice (Fig 7A). B20-4.1.1 treatment did not alter the numbers of CD11b^{+VE} cells within the lungs of mice injected intravenously with fs120-LS cells at 48 h (Figure 7B). These results show that the presence of fs120-LS cells but not fs188-LS cells in lung tissue leads to an increase in CD11b^{+VE} immune cells that is dependent on VEGFR1 stromal activity.

Discussion

We have found that metastasis of fibrosarcomas to the lung from subcutaneous tumors is strongly influenced by which isoforms of VEGFA are expressed by the cancer cells, with the more soluble isoforms associated with increased metastasis. Moreover, results clearly showed that tumor cells expressing VEGF120 versus VEGF188 had increased survival in the lung 48 h after intravenous injection and that the presence of a VEGF120-expressing primary tumor enhanced this effect. Survival of fs120-LS tumor cells in the lung after 48 h was associated with stromal activity of VEGFR1 yet was not influenced by inhibition of VEGFA itself using the antibody B20-4.1.1. In contrast, B20-4.1.1 did significantly decrease lung metastasis from primary fs120-LS subcutaneous

tumors, with an insignificant effect on fs188-LS tumors (summarized in Supplementary Fig S8).

Our previous studies in mice have shown that expression of short isoforms of VEGFA (120/164) lead to changes in the primary tumor microenvironment known to associate with metastasis including reduced pericyte coverage and increased interstitial fluid pressure (IFP) (12,13); important factors influencing cell survival during metastasis (15,29). In addition, our studies *in vitro* have shown that VEGF188 expressing tumor cells have increased levels of apoptosis and decreased proliferation compared with VEGF120 expressing cells (24). In the current study, we show that VEGF120 expressing cells have increased survival and proliferation in the lung following intravenous injection. A recent study published by Benedetto *et al* showed that VEGF189 overexpression in human MDA-MB-231 breast cancer cells increased apoptosis and decreased establishment of experimental lung metastases in mice after intravenous injection (30). Our current results are consistent with these data and furthermore show that differential effects of the isoforms on lung metastasis are apparent when VEGFA in tumor cells is under the control of its constitutive promoter, ensuring physiological regulation of its production.

We were able to identify at which point metastasis is sensitive to anti-VEGFA therapy by comparing metastasis to the lung from subcutaneous tumors with tumor cell survival after intravenous injection. VEGF120 expression led to increased lung metastasis from subcutaneous tumors, which was *sensitive* to B20-4.1.1, and increased survival of tumor cells after intravenous injection,

which was *insensitive* to B20-4.1.1. We found no VEGFA isoform selective effect of B20-4.1.1 on subcutaneous tumor growth, vascular density or pericyte investment that could account for the preferential effect of B20-4.1.1 on fs120-LS tumor metastasis from the subcutaneous site, although the antibody did significantly decrease vascular density in both fs120-LS and fs188-LS subcutaneous tumors, which is likely to have contributed to the anti-metastatic effect observed in the fs120-LS tumors. Characterization of the ECM within subcutaneous tumors revealed differences in laminin versus collagen-I content, with fs120-LS tumors having higher levels of laminin and lower levels of collagen-I compared to fs188-LS tumors. The distribution of laminin and collagen was also different between fs120-LS and fs188-LS tumors, with laminin and collagen having a greater degree of association with the vasculature in fs188-LS tumors. This is consistent with increased vascular maturation and decreased vascular permeability in fs188-LS tumors (12), which could contribute to their lower metastatic propensity. Laminin was expressed at higher levels in fs120-LS tumors compared to fs188-LS tumors and was distributed throughout the tumor tissue not just localized to the vasculature. Migration of fs188 cells on both laminin and collagen *in vitro* was insensitive to B20-4.1.1. In contrast, fs120 cell's migration on laminin, but not collagen, was sensitive to B20-4.1.1. Considering the widespread prominence of laminin in fs120-LS tumours, this could at least partially explain the particular sensitivity of this tumor type to the anti-metastatic effect of B20-4.1.1. Why fs120 cells have a dependence on VEGFA for migration on laminin requires further investigation. Interaction between VEGFA, VEGF receptors and the co-receptor neuropilin-1 (NRP1) can regulate migration and this has been reported to be VEGFA isoform

dependent in some cell types (3,31,32). Such a selectivity of interaction could be involved in our observations, since our previous studies have shown that fs120 and 188 cells express VEGFR1 and 2 and NRP1 to varying extents (24).

In addition to effects in the primary tumor, we also identified that there was increased survival of fs120 versus fs188 cells within the lung 48 h after intravenous injection, which was insensitive to treatment with B20-4.1.1. There were also more fs120-LS cells arrested within the lung vasculature in the first 5 min after intravenous injection compared with fs188-LS cells. Previous long-standing studies have shown that overcoming the initial trauma of forces associated with capillary arrest is a significant rate-limiting step in metastasis (26). Correlations between increased metastasis and greater cell deformability are also well established (33,34) and more recently this has been linked to activation of γ H2AX phosphorylation, a marker commonly used to detect DNA damage (27). Our data indicate that fs120-LS cells have greater resistance to trauma incurred through vascular arrest than fs188-LS cells, demonstrated by lower activation of the DNA damage marker p- γ H2AX. Consistent with the *in vitro* characteristics of the tumor cells (24), the proportion of proliferative tumor cells in the lung, within the first 48 h after intravenous injection, was significantly greater for fs120-LS than fs188-LS cells. We have previously shown fs120 cells have greater actinomyosin contractility and display a more amoeboid morphology *in vitro*, unlike fs188 cells that display more orthodox mesenchymal features (24). This could explain the increased capacity of fs120 cells to resist mechanical trauma during circulation and capillary arrest. Furthermore fs120 cells exhibit greater plasticity and can shift between amoeboid and mesenchymal

states (23), a characteristic that also potentially favors their escape through matrix barriers (35). Relatively long-term adaptive changes within the tumor cells to expression of a single VEGFA isoform leading to these differences between fs120 and fs188 cells could explain why treatment with B20-4.1.1 over the 48 h examined in this study could not inhibit survival of intravenously-injected luciferase expressing cells within the lung. Further studies are required to investigate these processes.

Survival of tumor cells in the lung can be supported by recruitment of CD11b cells (28,36); a process that is also dependent on stromal VEGFR1 (20,28). We found that intravenous injection of fs120 cells, but not fs188 cells, increased levels of CD11b cells in the lung at 48 h and this was dependent on stromal VEGFR1 activity. VEGFR1 dependency was also seen on metastasis to the lung from subcutaneous fs120 tumors, although in this case there were clearly additional primary tumor-related factors influencing metastatic spread, as the presence of a subcutaneous fs120 tumor also increased 48 h survival of intravenously injected cells in the lung. Although an increase in plasma VEGFA and PIGF2 was detected in mice bearing fs120-LS tumors, we could not replicate the 48 h-survival effect by injecting conditioned medium as reported in the literature in other model systems (28,37). We cannot rule out the possibility that the primary tumor releases other tumor-derived factors that are not present in cell-conditioned medium, such as exosomes, growth factors or cells derived from the activated stroma (38). However, metastasis of fs120-LS cells to the lung from subcutaneous fs120-LS tumors was an early event, suggesting that cells already within the lung may increase survival of cells that arrive subsequently. The

function-blocking VEGFA antibody, B20-4.1.1 had no effect on survival of intravenously injected cells in the lung and did not inhibit the increase in CD11b cells. This re-enforces our data showing B20-4.1.1 inhibits VEGF120-dependent processes predominantly in the subcutaneous primary tumor for its anti-metastatic effect, as well as re-enforcing a role for VEGF120 expression in conferring fibrosarcoma cells with additional advantages during the early stages of survival within the tissue of the lung that are not sensitive to anti-VEGFA therapy. As our data show, there is a high degree of redundancy in VEGFR1 ligands in mice with VEGF120 expressing tumors, particularly in plasma and lung tissue, hence targeting VEGFR1 directly may inhibit survival of disseminated cells within the lung, as found in previous studies of other tumor types (39,40). In a pilot study, we found that treatment with the VEGFR1/2 tyrosine kinase inhibitor cediranib tended to decrease survival of fs120-LS cells within the lung 48 h after intravenous injection but this effect was not statistically significant (Supplementary Fig S9). We conclude that either more selective or potent VEGFR1 inhibitors would be more effective or that further resistance mechanisms to VEGFA-VEGFR targeted therapies are present.

Overall, we conclude that VEGF120 expression confers a metastatic advantage over VEGF188 expression at several levels including high vascular density coupled to more immature, permeable vasculature in the primary tumor, increased vascular arrest and proliferation within the lung, leading to increased survival that is associated with VEGFR1-dependent recruitment of myeloid cells, possibly driven by multiple VEGFR1 ligands including VEGFA and PIGF2. Not all of these advantages in the metastatic cascade can be inhibited by anti-VEGFA

therapy, but we have identified the decrease in vascular density coupled to inhibition of cell migration as possible mechanisms by which anti-VEGFA therapy inhibits metastasis to the lung from subcutaneous primary fs120-LS tumors.

Our results support the clinical findings associating high levels of circulating soluble forms of VEGFA with poor prognosis in conjunction with a greater response to bevacizumab (Avastin®) and provide a mechanistic basis for these associations. Although the clinical associations were not significant in all settings (1) they were sufficiently promising for initiation of a phase III trial incorporating prospective analysis of plasma VEGFA levels in Her2^{VE} breast cancer to be initiated (MERiDiAN, NCT01663727/ G025632). VEGF pathway inhibitors are also becoming part of established treatment of soft tissue sarcoma (STS) following the PALETTE clinical trial (41). Other potential biomarkers of a good response to anti-VEGFA/VEGFR therapy include low levels of NRP-1 (2), which we previously found associated with VEGF120 tumor cell expression (24).

In summary, our data represents substantial progress in understanding the role of tumor VEGFA isoform expression in metastasis and points towards the utility of analyzing VEGFA isoform expression for predicting treatment outcome with bevacizumab. Furthermore, our results suggest that inhibition of VEGFR1 activity in combination with anti-VEGFA therapy may be particularly useful for treatment of tumors with high expression of soluble isoforms of VEGFA.

Acknowledgements

We would like to thank Genentech Inc. for the antibodies BE5 and B20-4.1.1 and Professors Shibuya and Plate for the VEGFR1-ΔTKD mice. We would also like to thank Susan Clark and Kay Hopkinson of the UoS Medical School flow cytometry core facility, Dr. Phil Watson and his team for assistance with fluorescence microscopy, Colin Gray for assistance with confocal microscopy, Maggie Glover and Jennifer Globe of the histology core facility, Dr Toby Holmes for his assistance with the IVIS Lumina II and the staff of the Biological Services Unit for their technical assistance.

References.

1. Jayson GC, Hicklin DJ, Ellis LM. Antiangiogenic therapy-evolving view based on clinical trial results. *Nat Rev Clin Onc* 2012;9(5):297-303.
2. Maru D, Venook AP, Ellis LM. Predictive biomarkers for bevacizumab: are we there yet? *Clin Cancer Res* 2013;19(11):2824-7.
3. Vempati P, Popel AS, Mac Gabhann F. Extracellular regulation of VEGF: isoforms, proteolysis, and vascular patterning. *Cyt Growth Fact Rev* 2014;25(1):1-19.
4. Ferrara N. Binding to the extracellular matrix and proteolytic processing: two key mechanisms regulating vascular endothelial growth factor action. *Mol Biol Cell* 2010;21(5):687-90.
5. Van Cutsem E, de Haas S, Kang YK, Ohtsu A, Tebbutt NC, Ming Xu J, et al. Bevacizumab in Combination With Chemotherapy As First-Line Therapy in Advanced Gastric Cancer: A Biomarker Evaluation From the AVAGAST Randomized Phase III Trial. *J Clin Onc* 2012;30(17):2119-27.
6. Miles DW, de Haas SL, Dirix LY, Romieu G, Chan A, Pivot X, et al. Biomarker results from the AVADO phase 3 trial of first-line bevacizumab plus docetaxel for HER2-negative metastatic breast cancer. *Brit J Cancer* 2013;108(5):1052-60.
7. Lambrechts D, Lenz HJ, de Haas S, Carmeliet P, Scherer SJ. Markers of response for the antiangiogenic agent bevacizumab. *Journal of clinical oncology : official journal of the American Society of Clinical Oncology* 2013;31(9):1219-30.
8. Paule B, Bastien L, Deslandes E, Cussenot O, Podgorniak MP, Allory Y, et al. Soluble isoforms of vascular endothelial growth factor are predictors

- of response to sunitinib in metastatic renal cell carcinomas. PLoS One 2010;5(5):e10715.
9. Santos LV, Cruz MR, Lopes Gde L, Lima JP. VEGF-A levels in bevacizumab-treated breast cancer patients: a systematic review and meta-analysis. Breast Cancer Res Treat 2015;151(3):481-9.
 10. Carmeliet P, Ng YS, Nuyens D, Theilmeier G, Brusselmans K, Cornelissen I, et al. Impaired myocardial angiogenesis and ischemic cardiomyopathy in mice lacking the vascular endothelial growth factor isoforms VEGF164 and VEGF188. Nat Med 1999;5(5):495-502.
 11. Stalmans I, Ng YS, Rohan R, Fruttiger M, Bouche A, Yuce A, et al. Arteriolar and venular patterning in retinas of mice selectively expressing VEGF isoforms. J Clin Invest 2002;109(3):327-36.
 12. Tozer GM, Akerman S, Cross NA, Barber PR, Bjorndahl MA, Greco O, et al. Blood vessel maturation and response to vascular-disrupting therapy in single vascular endothelial growth factor-A isoform-producing tumors. Cancer Res 2008;68(7):2301-11.
 13. Akerman S, Fisher M, Daniel RA, Lefley D, Reyes-Aldasoro CC, Lunt SJ, et al. Influence of soluble or matrix-bound isoforms of vascular endothelial growth factor-A on tumor response to vascular-targeted strategies. Int J Cancer 2013;133(11):2563-76.
 14. Cooke VG, LeBleu VS, Keskin D, Khan Z, O'Connell JT, Teng Y, et al. Pericyte depletion results in hypoxia-associated epithelial-to-mesenchymal transition and metastasis mediated by met signaling pathway. Cancer Cell 2012;21(1):66-81.

15. Lunt SJ, Chaudary N, Hill RP. The tumor microenvironment and metastatic disease. *Clin Exp Met* 2009;26(1):19-34.
16. Workman P, Aboagye EO, Balkwill F, Balmain A, Bruder G, Chaplin DJ, et al. Guidelines for the welfare and use of animals in cancer research. *Brit J Cancer* 2010;102(11):1555-77.
17. Hiratsuka S, Minowa O, Kuno J, Noda T, Shibuya M. Flt-1 lacking the tyrosine kinase domain is sufficient for normal development and angiogenesis in mice. *Proc Nat Acad Sci* 1998;95(16):9349-54.
18. Bagri A, Berry L, Gunter B, Singh M, Kasman I, Damico LA, et al. Effects of anti-VEGF treatment duration on tumor growth, tumor regrowth, and treatment efficacy. *Clin Cancer Res* 2010;16(15):3887-900.
19. Liang WC, Wu X, Peale FV, Lee CV, Meng YG, Gutierrez J, et al. Cross-species vascular endothelial growth factor (VEGF)-blocking antibodies completely inhibit the growth of human tumor xenografts and measure the contribution of stromal VEGF. *J Biol Chem* 2006;281(2):951-61.
20. Hiratsuka S, Nakamura K, Iwai S, Murakami M, Itoh T, Kijima H, et al. MMP9 induction by vascular endothelial growth factor receptor-1 is involved in lung-specific metastasis. *Cancer cell* 2002;2(4):289-300.
21. Dawson MR, Duda DG, Chae SS, Fukumura D, Jain RK. VEGFR1 activity modulates myeloid cell infiltration in growing lung metastases but is not required for spontaneous metastasis formation. *PLoS One* 2009;4(9):e6525.
22. Friedrich J, Seidel C, Ebner R, Kunz-Schughart LA. Spheroid-based drug screen: considerations and practical approach. *Nat Prot* 2009;4(3):309-24.

23. Pickup MW, Mouw JK, Weaver VM. The extracellular matrix modulates the hallmarks of cancer. *EMBO Rep* 2014;15(12):1243-53.
24. Kanthou C, Dachs GU, Lefley DV, Steele AJ, Coralli-Foxon C, Harris S, et al. Tumour cells expressing single VEGF isoforms display distinct growth, survival and migration characteristics. *PLoS One* 2014;9(8):e104015.
25. Kalluri R, Zeisberg M. Fibroblasts in cancer. *Nat Rev* 2006;6(5):392-401.
26. Weiss L. Biomechanical interactions of cancer cells with the microvasculature during hematogenous metastasis. *Cancer Met Rev* 1992;11(3-4):227-35.
27. Denais CM, Gilbert RM, Isermann P, McGregor AL, te Lindert M, Weigelin B, et al. Nuclear envelope rupture and repair during cancer cell migration. *Science* 2016;352(6283):353-8.
28. Kaplan RN, Riba RD, Zacharoulis S, Bramley AH, Vincent L, Costa C, et al. VEGFR1-positive haematopoietic bone marrow progenitors initiate the pre-metastatic niche. *Nature* 2005;438(7069):820-7.
29. Kim JW, Wong CW, Goldsmith JD, Song C, Fu W, Allion MB, et al. Rapid apoptosis in the pulmonary vasculature distinguishes non-metastatic from metastatic melanoma cells. *Cancer Lett* 2004;213(2):203-12.
30. Di Benedetto M, Toullec A, Buteau-Lozano H, Abdelkarim M, Vacher S, Velasco G, et al. MDA-MB-231 breast cancer cells overexpressing single VEGF isoforms display distinct colonisation characteristics. *Brit J Cancer* 2015;113(5):773-85.
31. Pan Q, Chathery Y, Wu Y, Rathore N, Tong RK, Peale F, et al. Neuropilin-1 binds to VEGF121 and regulates endothelial cell migration and sprouting. *J Biol Chem* 2007;282(33):24049-56.

32. Banerjee S, Mehta S, Haque I, Sengupta K, Dhar K, Kambhampati S, et al. VEGF-A165 induces human aortic smooth muscle cell migration by activating neuropilin-1-VEGFR1-PI3K axis. *Biochemistry* 2008;47(11):3345-51.
33. Zhang W, Kai K, Choi DS, Iwamoto T, Nguyen YH, Wong H, et al. Microfluidics separation reveals the stem-cell-like deformability of tumor-initiating cells. *Proc Nat Acad Sci* 2012;109(46):18707-12.
34. Ochalek T, Nordt FJ, Tullberg K, Burger MM. Correlation between cell deformability and metastatic potential in B16-F1 melanoma cell variants. *Cancer Res* 1988;48(18):5124-8.
35. Friedl P, Alexander S. Cancer invasion and the microenvironment: plasticity and reciprocity. *Cell* 2011;147(5):992-1009.
36. Hiratsuka S, Watanabe A, Aburatani H, Maru Y. Tumour-mediated upregulation of chemoattractants and recruitment of myeloid cells predetermines lung metastasis. *Nat Cell Biol* 2006;8(12):1369-75.
37. Erler JT, Bennewith KL, Cox TR, Lang G, Bird D, Koong A, et al. Hypoxia-induced lysyl oxidase is a critical mediator of bone marrow cell recruitment to form the premetastatic niche. *Cancer Cell* 2009;15(1):35-44.
38. Peinado H, Lavotshkin S, Lyden D. The secreted factors responsible for pre-metastatic niche formation: old sayings and new thoughts. *Semin Cancer Biol* 2011;21(2):139-46.
39. Qian BZ, Zhang H, Li J, He T, Yeo EJ, Soong DY, et al. FLT1 signaling in metastasis-associated macrophages activates an inflammatory signature that promotes breast cancer metastasis. *J Exp Med* 2015;212(9):1433-48.

40. Cicatiello V, Apicella I, Tudisco L, Tarallo V, Formisano L, Sandomenico A, et al. Powerful anti-tumor and anti-angiogenic activity of a new anti-vascular endothelial growth factor receptor 1 peptide in colorectal cancer models. *Oncotarget* 2015;6(12):10563-76.
41. van der Graaf WT, Blay JY, Chawla SP, Kim DW, Bui-Nguyen B, Casali PG, et al. Pazopanib for metastatic soft-tissue sarcoma (PALETTE): a randomised, double-blind, placebo-controlled phase 3 trial. *Lancet* 2012;379(9829):1879-86.

Figure Legends.

Figure 1. Fibrosarcomas expressing VEGF120 have increased metastasis to the lung compared to those expressing VEGF188. In A and B, mice were subcutaneously injected with 1×10^6 fs120-LS, fs164-LS, fs188-LS or fsWT-LS cells and tumors grown to 1000 mm^3 (end-point size). In C-F, mice were injected intravenously via the tail vein with 5×10^4 cells and experimental metastasis monitored live or *ex vivo* using bioluminescence. **A.** Lungs were removed when primary subcutaneous tumors reached their end-point size and luciferase activity measured in whole lung homogenates, as photons per second per μg protein extracted (p/s/ μg). Background bioluminescence of lungs from normal mice is shown as ‘Normal Lung’. Each symbol represents a lung homogenate from an individual mouse ($n = 6$ for normal and 21-23 for fs120, 164, 188 and WT-LS). Data are from three independent cohorts, normalized against the mean bioluminescence for WT-LS. **B.** Kaplan-Meier plots of the percentage of mice with tumors less than the end-point size versus time after subcutaneous tumor cell injection. fsWT-LS tumors took a small but significantly longer time to reach the end-point size compared to fs120-LS and fs164-LS tumors ($p = 0.025$ and 0.041 respectively), with no significant difference between other groups ($n = 16-18$). **C and D.** Example images of experimental lung metastases at day 21 after intravenous injection of fs120-LS or fs188-LS cells (2 mice for each cell type). Bioluminescence is shown as false color images overlaid onto the black and white images of live mice (**C**) or excised lung lobes (**D**). **E.** Quantification of bioluminescence from the thoracic region of live mice 21 days after intravenous injection ($n = 9-12$). **F.** Kaplan-Meier plots of the percentage of mice with lung bioluminescence less than 1×10^7 p/s (humane end-point, surrogate for

survival) versus time after intravenous injection ($n = 9-12$). Error bars are \pm SEM. $P < 0.01 = **$, $< 0.001 = ***$, NS = Not Significant.

Figure 2. Metastasis of fs120-LS cells to the lung from subcutaneous tumors differs in sensitivity to anti-VEGFA therapy and host VEGFR1 activity in comparison to survival after intravenous injection. **A.** Mice were injected subcutaneously with either 1×10^6 fs120-LS or fs188-LS cells and tumors grown to 200 mm^3 before treatment with 5 mg/kg B20-4.1.1 or control IgG twice weekly until tumor end point volume of 1000 mm^3 . Luciferase activity in lung lysates was measured and corrected for protein extracted, as described for Fig 1. Each symbol represents a lung homogenate from an individual mouse ($n = 12-20$). **B.** Mice were injected with 1×10^6 fs120-LS or fs188-LS cells and tumors grown to 1000 mm^3 before plasma was collected and VEGFA measured by ELISA and compared to control plasma ($n = 9-13$ in each group). **C.** VEGFR1-WT or Δ TKD mice were subcutaneously injected with 1×10^6 fs120-LS or fs188-LS cells and tumors grown to 1000 mm^3 (end-point size). Luciferase activity was measured in whole lung homogenates of mice corrected for protein extracted, as above. Each symbol represents data from an individual mouse ($n = 21-23$). Data are from three independent cohorts, normalized against the mean bioluminescence for fs188-LS in VEGFR1-WT mice. **D and E.** VEGFR1-WT or VEGFR1- Δ TKD mice were injected intravenously with 5×10^4 fs120-LS or fs188-LS cells ($n = 11-12$ in each group). Example images of fs120-LS cell bioluminescence in excised lung lobes of VEGFR1-WT and VEGFR1- Δ TKD mice (D) and measurement of bioluminescence on necropsy (E) of intact lung lobes after 48 h are shown. Data are from three independent cohorts, normalized against the mean bioluminescence for fs188-LS

in VEGFR1-WT mice. **F.** Mice were first injected with control IgG or B20-4.1.1 at 5 mg/kg. After 48 h mice received a further injection of antibody at the same time as intravenous injection of fs120-LS cells, with intact lung lobe bioluminescence analyzed after a further 48 h ($n = 7$ in each group). Error bars are \pm SEM. $P < 0.05$ = *, $< 0.01 = **$, $< 0.001 = ***$, NS = Not Significant.

Figure 3. Subcutaneous fs120 tumors enhance survival of intravenously injected fs120-LS cells in the lung. **A.** VEGFR1-WT or VEGFR1-ΔTKD mice were injected subcutaneously with 1×10^6 fs120 or fs188 cells and then received intravenous injections of fs120-LS or fs188-LS cells respectively when subcutaneous tumors reached 200 mm^3 . Bioluminescence of excised intact lung lobes was analyzed 48 h after intravenous injection of cells ($n = 11 - 18$). Data is from 2 independent cohorts normalized against bioluminescence of fs188/188-LS cells in VEGFR1-WT mice. **B.** Alternatively, when subcutaneous fs120 tumors in VEGFR1-WT mice reached 200 mm^3 , B20-4.1.1 or control IgG was first administered. After 48 h mice received a further injection of antibody at the same time as intravenous injection of fs120-LS cells, with excised intact lung lobe bioluminescence analyzed after a further 48 h ($n = 6-8$). **C.** fs120-LS and fs188-LS cells were cultured in T25 flasks at 60 – 70% confluence in 3 ml of fresh medium and incubated overnight in either atmospheric O₂ or 1% O₂. PIGF2 levels in cell-conditioned medium were quantified using ELISA ($n = 3$). **D.** Mice were injected subcutaneously with 1×10^6 fs120-LS or fs188-LS cells and tumors grown to 1000 mm^3 before plasma was collected and PI GF2 measured by ELISA and compared to control plasma ($n = 8-10$ in each group). **E.** Mice were injected with 1×10^6 fs120-LS or fs188-LS cells subcutaneously and tumors grown to 1000 mm^3 .

mm^3 before lungs were removed, homogenized and supernatants analyzed for PIGF2 by ELISA and compared to control lungs (control n = 6, tumor bearing mice n = 13 - 22). Error bars are $\pm \text{SEM}$. P < 0.05 = *, p < 0.01 = **, p < 0.001 = ***, NS = Not Significant.

Figure 4. fs120-LS and fs188-LS subcutaneous tumors both respond to anti-VEGFA treatment. **A - B.** Mice were injected subcutaneously with either 1×10^6 fs120-LS or fs188-LS and tumors grown to 200 mm^3 before treatment with 5 mg/kg B20-4.1.1 or control IgG twice weekly and tumor volume measured to end-point with arrows indicating injection time points (end point $>1000 \text{ mm}^3$, n = 10 - 11). **C.** Tumor volume as percent control IgG mean tumor volume for fs120-LS and fs188-LS tumors respectively measured 48 h after tumors had received 2 injections of control IgG or B20-4.1.1 (n = 10 - 11). **D - E.** FFPE sections of tumors were stained for CD31 and counter-stained with hematoxylin (D) and mean vascular density counted using random high-powered fields of view (20 x) within viable tumor regions (E) (n = 11-12 in each group). Scale bar is 100 μm . **F.** Example immunofluorescence images of FFPE tumor sections stained with anti-CD34 (red) and anti α SMA (green) identifying α SMA^{+VE} perivascular cells (solid arrowheads) and non-perivascular stromal cells (open arrowheads). Scale bar is 20 μm . **G.** Mean density of α SMA positive vessels in sections from F (n = 6). Error bars are $\pm \text{SEM}$. P < 0.05 = *, < 0.01 = **, < 0.001 = ***, NS = Not Significant.

Figure 5. Fibrosarcomas expressing VEGF120 generate tumors with high levels of laminin that promotes VEGFA-dependent migration. **A and B.** Densitometric quantification of laminin (A) or collagen-I (B) levels from fs120 or fs188 from

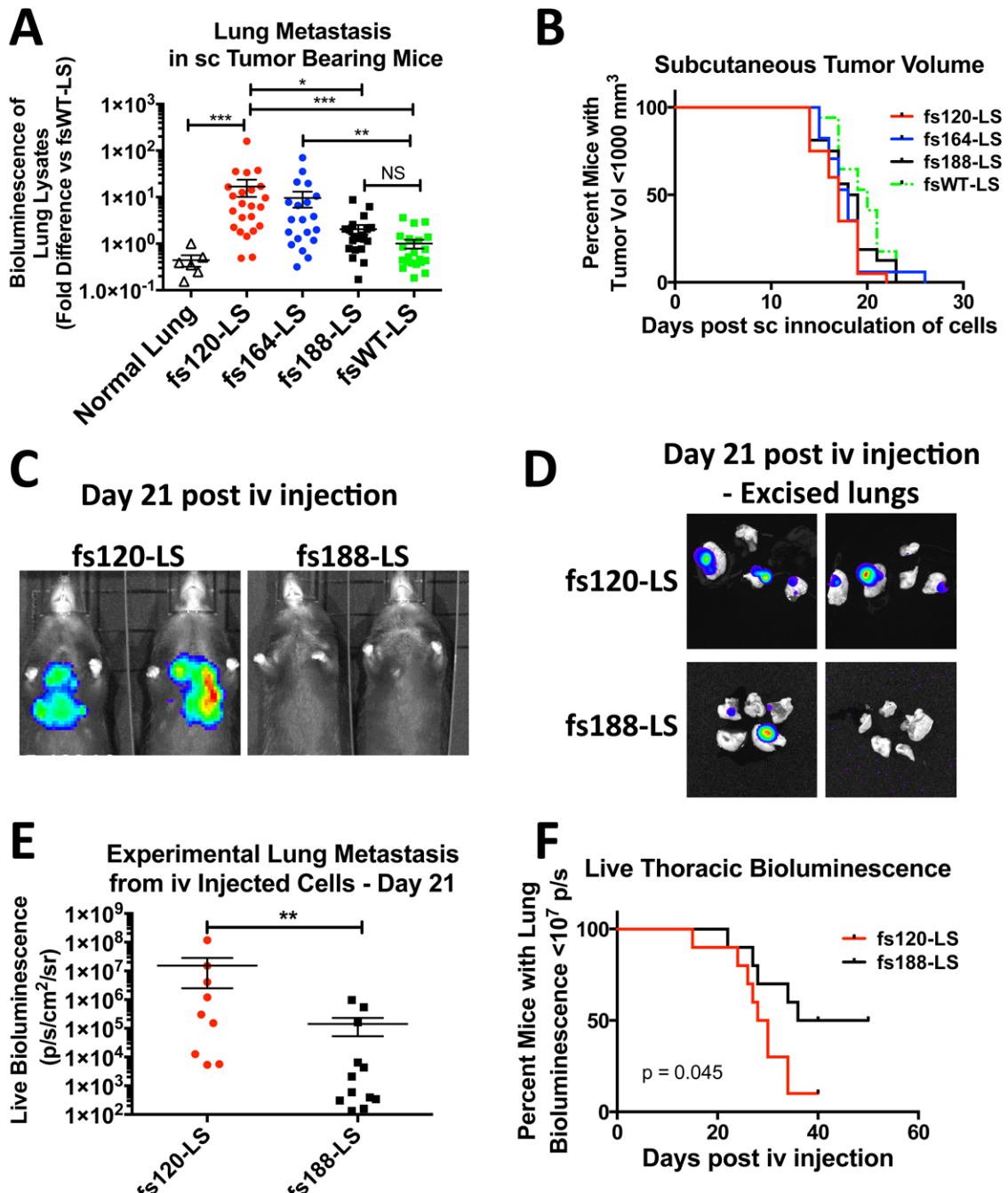
tumor lysates normalized for GAPDH ($n = 4$) together with representative blots of laminin, collagen-I and GAPDH detected in tumor lysates. Molecular sizes (kDa) are indicated on the left hand side of each blot. **C.** Immunofluorescence co-staining of laminin in frozen sections of fs120-LS and fs188-LS tumors. Grey scale images are shown for laminin and CD31 with the color merged image below showing laminin (green), CD31 (red) and nuclei (blue). Scale bar = 150 μm . **D.** Immunofluorescence co-staining of collagen-I in frozen sections of fs120-LS and fs188-LS tumors. Grey scale images are shown for collagen and CD31 with the color merged image below showing collagen (green), CD31 (red) and nuclei (blue). Scale bar = 150 μm . **E and F.** Migration of fs120 or fs188 cells across laminin (E) or collagen-I (F) coated transwell membranes in the presence of 10 $\mu\text{g}/\text{ml}$ B20-4.1.1 or control IgG. Data are the mean \pm SEM of 4 replicates and representative of 3 independent experiments. Error bars are \pm SEM. $P < 0.05$ = *, $< 0.01 = **$, $< 0.001 = ***$, NS = Not Significant.

*Figure 6. fs120-LS cells have an advantage over fs188-LS during vascular arrest and subsequent proliferation in the lung. **A.** Bioluminescence of intact lung lobes was analyzed 5 min and 48 h after intravenous injection of fs120-LS or fs188-LS cells ($n = 7 - 14$). **B.** Frozen sections of lungs 5 min after injection of cells shown in A were stained for SV40 to detect the fs-LS cells and the numbers of cells per random field of view were counted ($n = 5 - 6$). **C.** High-power example confocal images of SV40 positive cells (Red) showing rounded (left) and distorted (right) cells within the vasculature (CD31, green). A single confocal optical slice is shown. Scale bar is 15 μm . **D.** Example greyscale images of fs120-LS and fs188-LS cells within the lung; frozen sections stained for p- γ H2AX to detect DNA*

damage and SV40, with the color merged image showing p- γ H2AX in green, SV40 in red and nuclei in blue (DAPI). Scale bar is 20 μ m. **E.** Quantification of the number of SV40 and p- γ H2AX double positive cells per random field of view within the lung 5 min after intravenous injection ($n = 5 - 7$). **F.** Example greyscale images of fs120-LS and fs188-LS cells within the lung 48 h after intravenous injection; frozen sections stained for Ki67 as a marker of proliferation and SV40 to detect fs-LS cells and the color merged image with Ki67 in green, SV40 in red and nuclei in blue (DAPI). Scale bar is 20 μ m. **G.** Quantification of the number of SV40 and Ki67 double positive cells per random field of view within the lung 48 h after intravenous injection ($n = 7$). Error bars are \pm SEM. $P < 0.05 = ^*$, $< 0.01 = ^{**}$, $< 0.001 = ^{***}$, NS = Not Significant.

Figure 7. Survival of fs120-LS cells in the lung is associated with increased levels of CD11b cells. **A.** VEGFR1-WT or VEGFR1- Δ TKD mice were injected intravenously with 5×10^4 fs120-LS or fs188-LS cells and lungs removed after 5 min or 48 h. CD11b antigen positive (CD11b $^{+VE}$) cells were detected in frozen lung sections by immunofluorescence staining and counted from 5 random high-power fields of view (20 x objective) within alveolar regions with each data point representing the mean number of CD11b $^{+VE}$ cells per mouse ($n = 5 - 7$). **B.** Mice were treated on day 1 and 3 with 5 mg/kg B20-4.1.1 and injected with 5×10^4 fs120-LS cells intravenously before the mice were killed and the number of CD11b $^{+VE}$ cells within in frozen lung sections detected by immunofluorescence staining and counted as described in Fig 7A above ($n = 5 - 7$). Error bars are \pm SEM. $P < 0.001 = ^{***}$, NS = Not Significant.

Figure 1



D Day 21 post iv injection - Excised lungs

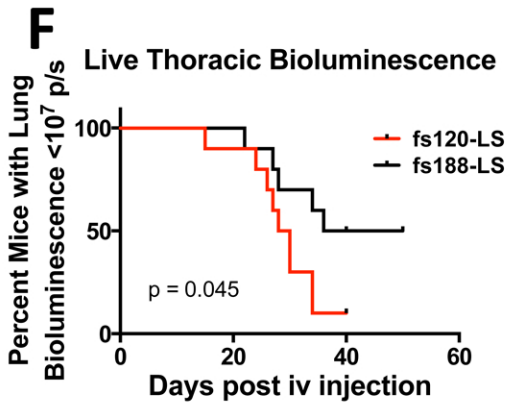
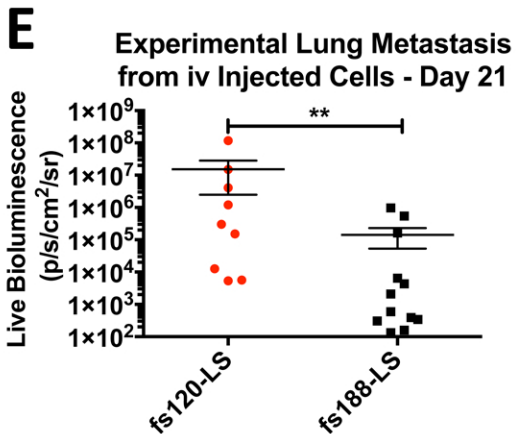
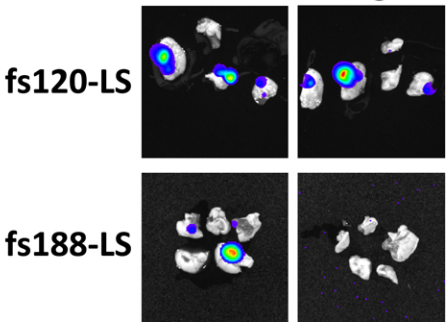


Figure 2

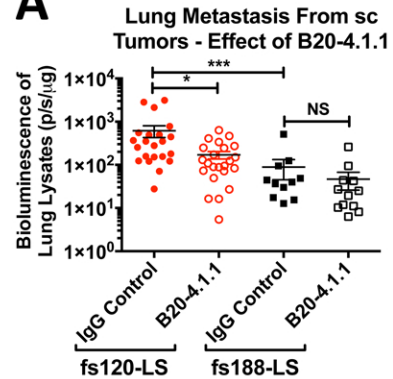
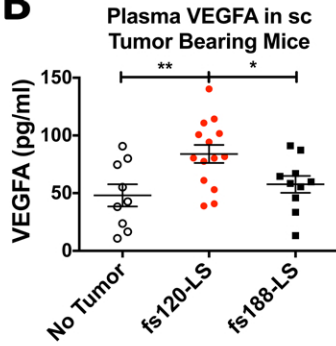
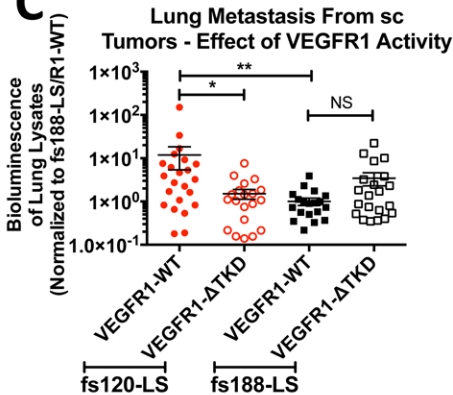
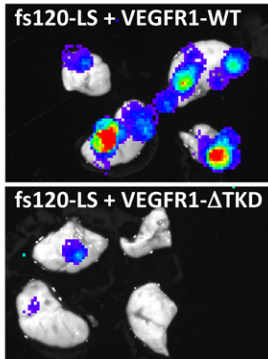
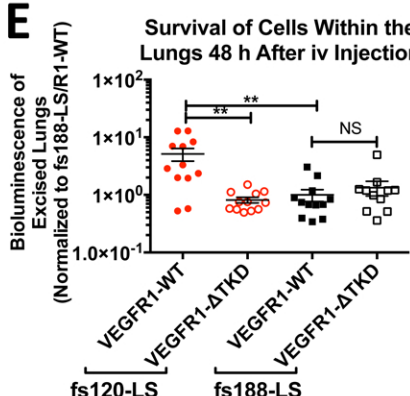
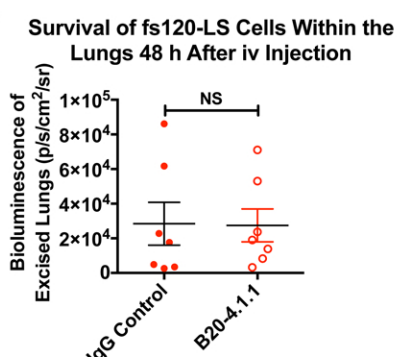
A**B****C****D****E****F**

Figure 3

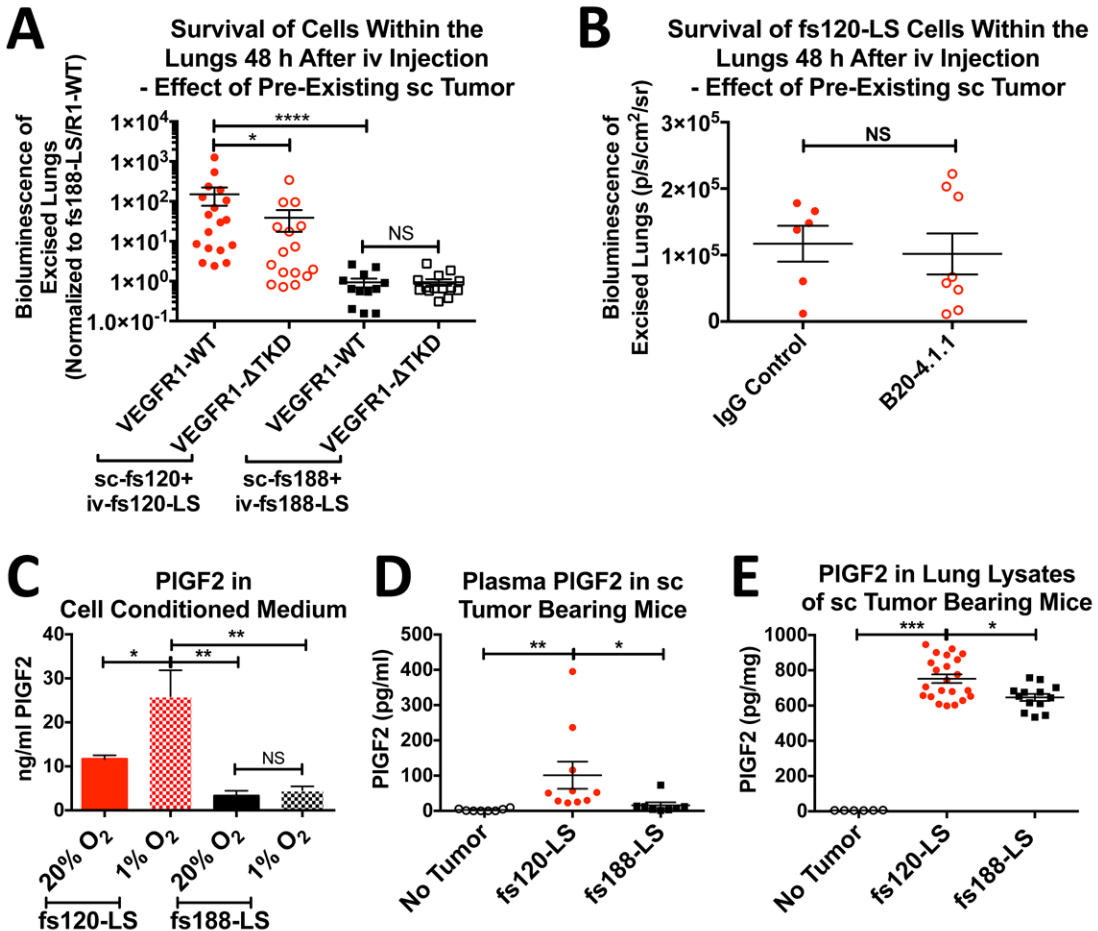


Figure 4

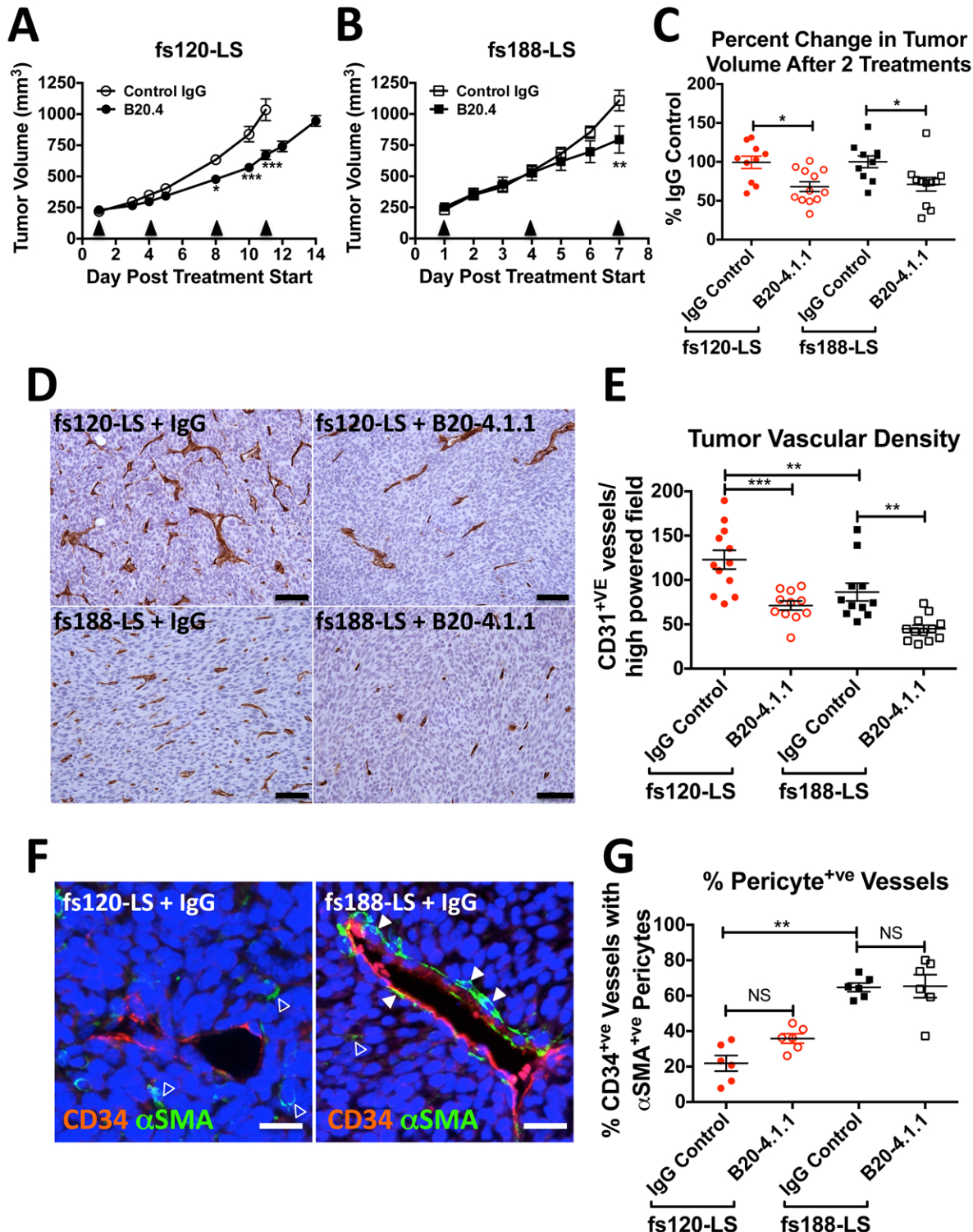


Figure 5

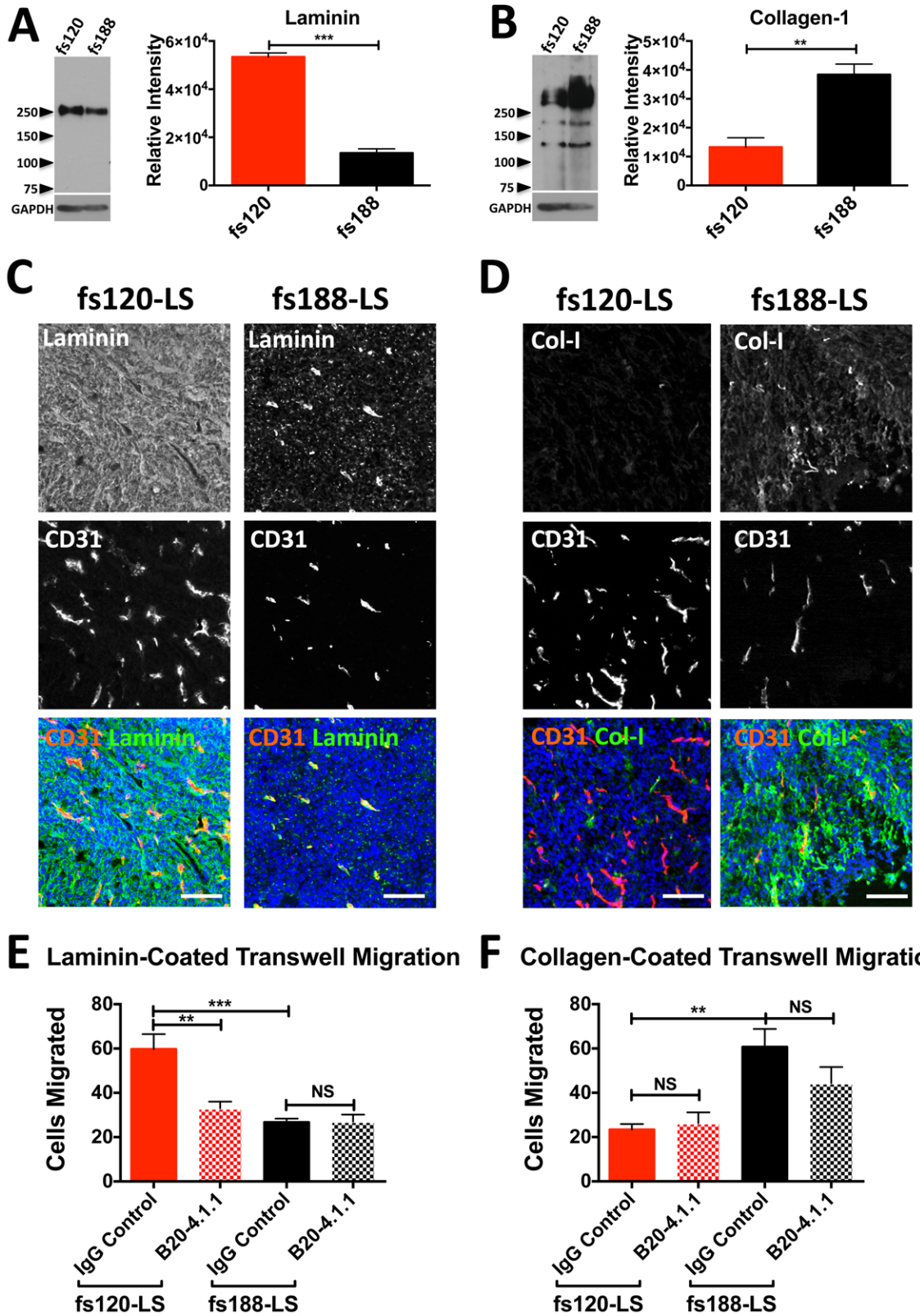


Figure 6

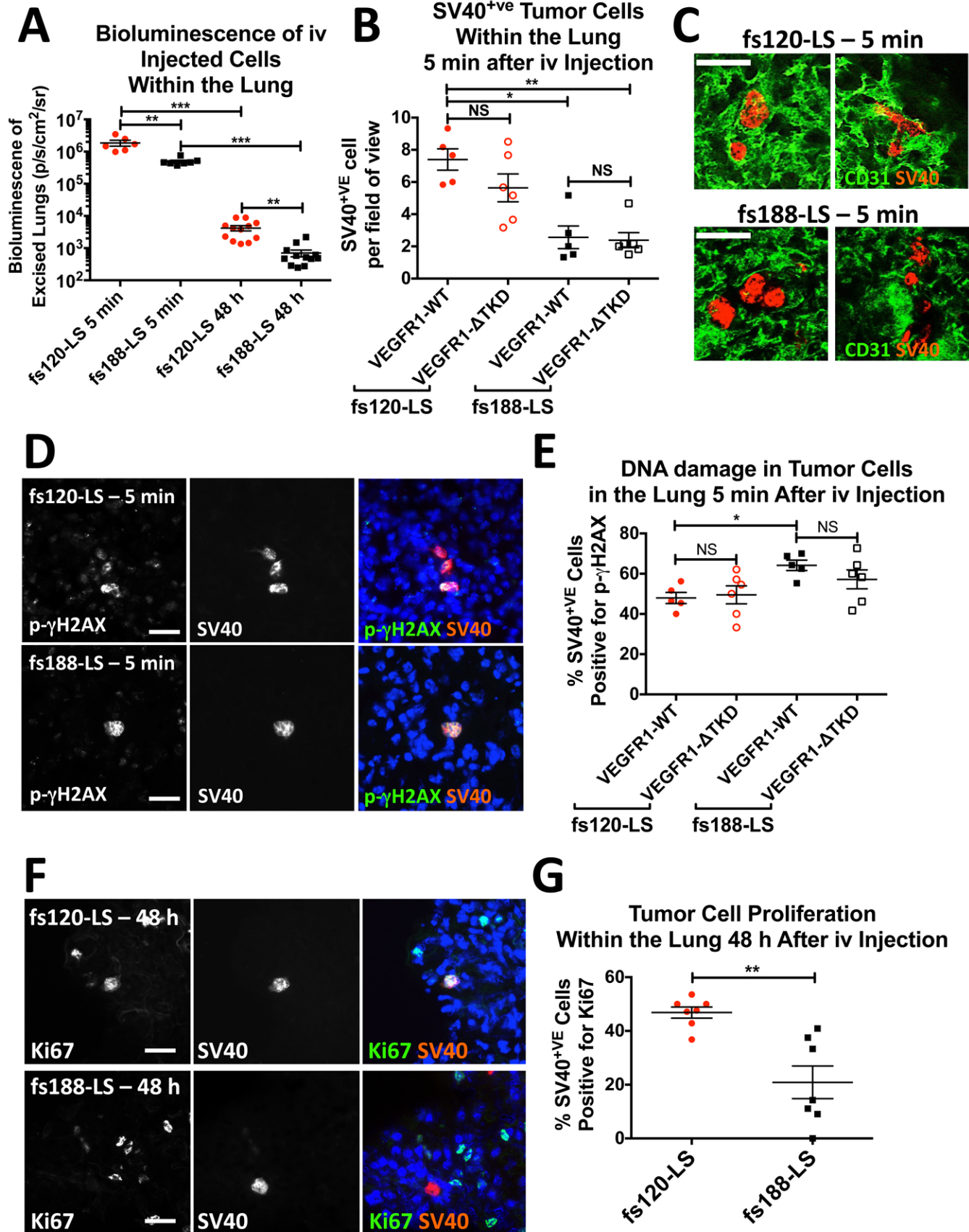


Figure 7

